Optical and Microwave Properties of Trivalent Chromium in β-Ga_2O_3

H. H. TIPPINS
Aerospace Corporation, El Segundo, California
(Received 27 August 1964)

Optical absorption, fluorescence, and paramagnetic-resonance experiments on single crystals of β-Ga_2O_3 doped with chromium were performed from room temperature down to a few degrees Kelvin. All the important low-lying energy levels have been identified from the optical data. The average positions of the three sets of sharp lines (doublet transitions) are almost identical to those of ruby, whereas the two prominent bands (quartet transitions) are broadened and shifted to the red for Ga_2O_3. Comparison of the 77°K absorption data with octahedral crystal-field calculations for the d^3 configuration yielded the values $B=700$ cm^{-1} and $Dq/B=2.35$. Fluorescence is observed from the ^2E to $^4A_2$ transition with a room-temperature lifetime of 0.23 msec. At 77°K these emission peaks occur at 6885 and 6956 Å. The fluorescence efficiency of crystals grown from different starting materials varied considerably, but the factors that give rise to this variation are only partly understood. The spin Hamiltonian parameters for the $^4A_2$ ground state were determined from X-band paramagnetic-resonance measurements and are: $D=-14.01$ kMc/sec, $E=+6.14$ kMc/sec, $g_x=1.978$, $g_y=1.978$, and $g_z=1.983$ for the z axis along [010]. The zero-field ground-state splitting was observed at a frequency of 35.18 kMc/sec. Calculations for the angular spectrum using this spin Hamiltonian are in excellent agreement with the X-band measurements. The possibility of using Cr^{3+} in Ga_2O_3 as the active material in an optical or microwave maser is briefly discussed.

I. INTRODUCTION

HOST materials for the study of trivalent transition metal ions are of considerable scientific interest. Gallium sesquioxide has the necessary optical and magnetic properties and should accept most of the trivalent iron group ions. Geller[1] has determined that the crystal structure of β-Ga_2O_3 is monoclinic and compares it with the α form, which is isostructural with α-Al_2O_3. So far, only β-Ga_2O_3 has been produced in single-crystal form, since it is the phase that is stable above about 800°C. Paramagnetic resonance studies on flux-grown samples of β-Ga_2O_3, doped with Cr^{3+}, were reported previously by Peter and Schawlow,[2] who concluded that the Cr^{3+} ions replace the Ga^{3+} ions in crystallographically equivalent octahedral sites. Presumably, the samples were very small and, except for the determination of the sign and magnitude of the ground-state splitting and the sign of the ^2E excited-state splitting, no optical data were reported. Recently, Chase has succeeded in growing large single crystals of β-Ga_2O_3 using the Verneuil technique.[3] Boules weighing several grams have been produced of the pure salt as well as of Cr^{3+} and Fe^{3+} doped material. A detailed investigation of the optical and microwave spectrum of the Cr^{3+} doped β-Ga_2O_3 has been performed, and the results of this investigation are presented in this paper. The X-band paramagnetic resonance measurements are in substantial agreement with the preliminary results of Peter and Schawlow and have resulted in a considerable improvement in the accuracy of the measured spin Hamiltonian parameters. The zero-field ground-state splitting was observed directly at a frequency of 35.18 kMc/sec. Both the optical absorption and fluorescence spectra were studied at several temperatures. All of the low-lying energy levels have been identified from the optical data.

Optical studies of the nominally pure β-Ga_2O_3 and Fe^{3+} doped material, as well as EPR studies of the latter, have also been performed and will be reported at a future time.

II. THEORY

Trivalent chromium, which has the electronic configuration d^3, has received considerable attention from both the theoretical and experimental standpoint. The

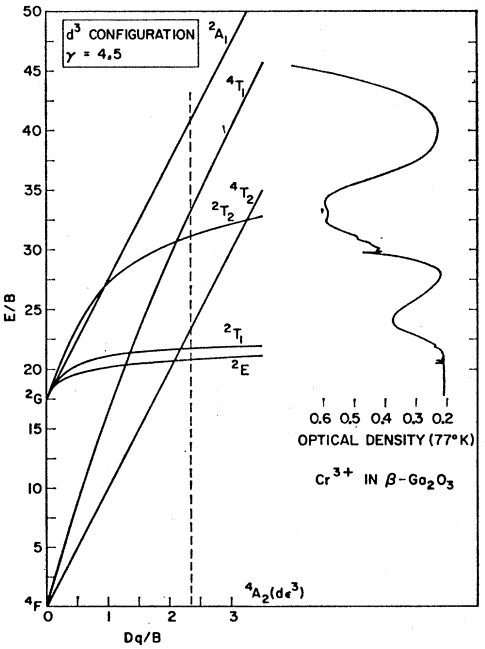

FIG. 1. Effect of an octahedral field on the states of the d^3 configuration [Tanabe and Sugano (Ref. 4)]. The 77°K absorption spectrum of Cr^{3+} in Ga_2O_3 is shown at the right for $B=700$ cm^{-1}.

[1] S. Geller, J. Chem. Phys. 33, 676 (1960).
[2] M. Peter and A. L. Schawlow, Bull. Am. Phys. Soc. 5, 158 (1960).
[3] A. Chase, J. Am. Ceram. Soc. 47, 470 (1964).

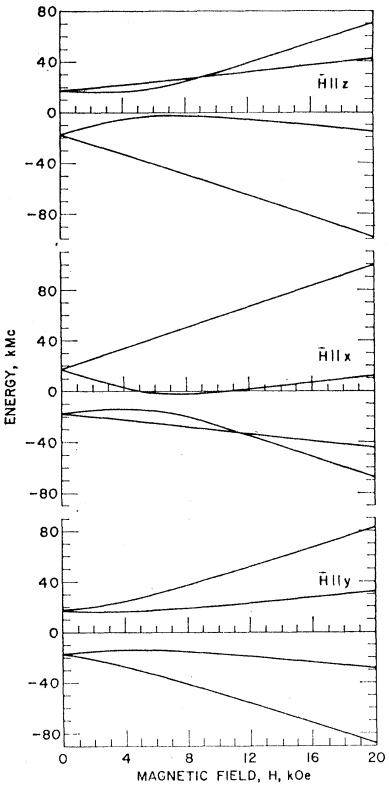

FIG. 2. Splitting of the $^4A_2$ ground-state energy levels of Cr^{3+} in Ga_2O_3 as a function of magnetic field.

influence of the crystalline field on the energy levels of transition metal ions has been treated in detail by Tanabe and Sugano.[4] The curves shown in Fig. 1 were obtained from the energy matrices given in this reference and illustrate the effect of a perfect octahedral field on the energy levels that arise from the d^3 configuration. For clarity, only those levels involved in ordinary optical transitions are shown. The symbol E denotes the energy, Dq is a measure of the strength of the crystal field, and B and C are the Racah parameters related to the standard radial integrals.[5] The ratio C/B, denoted by γ, was set equal to the constant value of 4.5. Near a Dq/B ratio of about 2.5, which applies for Cr^{3+} in Ga_2O_3, the states in order of increasing energy are

$$^4A_2(4),\ ^2E(4),\ ^2T_1(6),\ ^4T_2(12),\ ^2T_2(6),$$
$$^4T_1(12),\ \text{and}\ \ ^2A_1(2),$$

where the total degeneracy is given in parentheses following the state symbol. Much of the degeneracy is removed by fields of lower symmetry and the spin-orbit interaction; e.g., both the ground state and first excited state split into two doublets. Since these splittings are usually much smaller than that produced by the octahedral component of the crystalline field, the octahedral theory forms a useful first approximation for interpreting the optical data. Transitions from the ground state to quartet excited states produce characteristically broad and relatively strong absorption. Transitions from the ground state to excited doublet states arising from the same crystal-field configuration as the ground state produce sharp, weak absorptions.

The properties of the ground state are of particular interest and are conveniently studied by means of paramagnetic resonance. The ground-state splittings can be described by a spin Hamiltonian[6] with $S=\frac{3}{2}$, viz.,

$$\mathcal{H}=\beta(g_xH_xS_x+g_yH_yS_y+g_zH_zS_z)$$
$$+D(S_z^2-\tfrac{5}{4})+\tfrac{1}{2}E(S_+^2+S_-^2),$$

where D and E are the parameters that describe the crystal-field splitting, β is the Bohr magneton, and g is the spectroscopic splitting factor. For **H** parallel to one of the principal axes, the states couple in pairs and the solutions for energy as a function of H can be expressed in simple closed form. The fact that E is nonzero prevents the presentation of universal solutions in dimensionless form. The curves in Fig. 2, showing the splitting of the ground-state energy levels for **H** along the principal axes, were computed using the values of D and E determined from these experiments. The form of these curves is insensitive to the values of D and E. For comparison with experimental data, a much more useful computation is one that expresses the magnetic field H required for resonance at a fixed frequency versus the angle of **H** with respect to the crystallographic axes. The results of such a calculation for **H** in the plane perpendicular to the crystallographic b axis are shown in Fig. 3. The points on this graph represent experimental data, which are discussed in Sec. IV.

A special case of particular interest is the resonance frequencies for $H\cong 0$. For some materials, it is possible to observe a splitting of the ground state in the absence of a static magnetic field. A sweep field of a few hundred gauss is supplied by a set of Helmholtz coils, and the

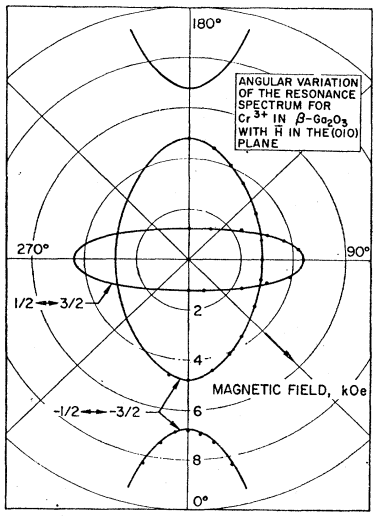

FIG. 3. Resonance fields at constant frequency for Cr^{3+} in Ga_2O_3. The solid curves were calculated from the spin Hamiltonian given in the text and for $f=9.636$ kMc/sec. The dots represent experimental data obtained at this frequency.

[4] Y. Tanabe and S. Sugano, J. Phys. Soc. Japan **9**, 753 (1954).
[5] D. S. McClure, Solid State Phys. **9**, 399 (1959).
[6] K. D. Bowers and J. Owen, Rept. Progr. Phys. **18**, 304 (1955).

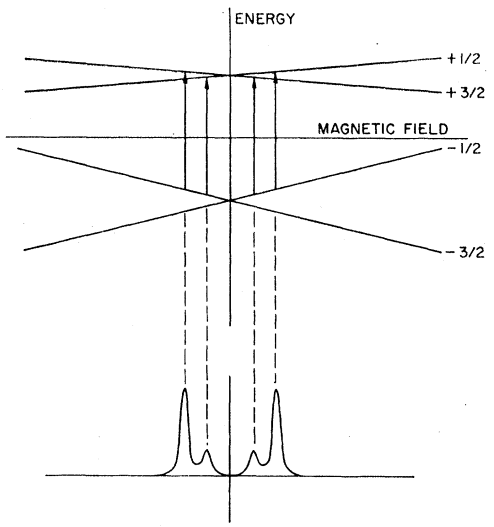

FIG. 4. Splitting of a quartet spin state in a weak magnetic field. The four resonances occurring for $f \gtrless W_0$ are indicated by the arrows.

microwave frequency is varied to search for the resonance. Details of this method are described in Sec. IV; however, it is mentioned here to point out that, in addition to the ground-state splitting, the spin Hamiltonian parameters D and E can be obtained from such an experiment. For **H** along the z axis, the energy levels are

$$\alpha \pm [(D+2\alpha)^2+3E^2]^{1/2}, \quad (1)$$

$$-\alpha \pm [(D-2a)^2+3E^2]^{1/2}, \quad (2)$$

where $\alpha = g_z\beta H/2$. For small H, terms higher than first order in H can be neglected, and the energy levels become

$$\tfrac{1}{2}W_0 \pm \alpha(1+4(D/W_0)), \quad (3)$$

$$-\tfrac{1}{2}W_0 \pm \alpha(1-4(D/W_0)), \quad (4)$$

where $W_0 = 2(D^2+3E^2)^{1/2}$ is the zero-field ground-state splitting. These energy levels for typical values of D and W_0 are shown in Fig. 4. The states are designated by their strong field quantum numbers. If it is assumed that the microwave frequency $f \gtrless W_0$, then, as indicated in Fig. 4, a resonance occurs for some small H due to the transition $E(-\frac{1}{2}) \rightarrow E(\frac{3}{2})$. The α that corresponds to this field H_1 is denoted by α_1. Similarly, for a slightly larger H, another resonance occurs when $E(\frac{1}{2})-E(-\frac{1}{2}) = f$. The α corresponding to this field H_2 is denoted by α_2. Two identical resonances occur for H in the opposite direction. From Eqs. (3) and (4), it follows that

$$f = W_0 + 8\alpha_1(D/W_0),$$
$$f = W_0 - 2\alpha_2.$$

Eliminating f gives

$$D = -(W_0/4)(H_2/H_1) \quad (5)$$

and the value of E follows from $W_0 = 2(D^2+3E^2)^{1/2}$. We therefore have the important result that, when W_0 has been determined, only one additional measurement is required to determine D and E. Furthermore, an absolute measurement of H is not necessary; only the ratio H_2/H_1 is required. For $f \gtrsim W_0$, the results are almost identical to those above. A similar analysis can be carried out for **H** along other axes, but the results are somewhat more complicated. The extension of this method to states with different values of S is straightforward. Although the accuracy of the method is limited, it has the advantages of simplicity and speed for determination of the spin Hamiltonian parameters.

III. APPARATUS

Both the X-band and R-band spectrometers used for these measurements are of conventional design and employ a magic-T bridge and crystal detector to observe the power reflected from the sample cavity. The klystron is stabilized on the sample cavity using a 10-kc automatic-frequency-control system. For the X-band measurements a 65-cps sweep field of approximately 200-G peak-to-peak is employed, and the resonance signal can be displayed directly on the oscilloscope. For small dilute samples, a 1-kc/sec sweep frequency was employed; the resulting signal is passed through a narrow-band amplifier and phase-sensitive detector and finally to a chart recorder, which displays the derivative curve of the resonance. The sample cavity is made of silver-plated brass and operates in the cylindrical TE_{111} mode. For this mode the sample is placed halfway up the side wall of the cavity (the point of maximum H_{rf}). The 12-in. electromagnet is mounted on a calibrated turntable so that the static field can be rotated in the plane perpendicular to H_{rf}.

For the zero-field R-band measurements the sample was mounted at the center of a tunable cylindrical cavity that operated in the TE_{011} mode. The cavity was located between a pair of 7-in.-diam Helmholtz coils that provided a sweep field of up to approximately 300-G peak-to-peak.

A cavity wavemeter was used for frequency measurements in both microwave systems. For the X-band system, the wavemeter was calibrated using a transfer oscillator and counter. For the R-band calibration, the transfer oscillator and counter were used to measure the frequency of a C-band oscillator, the fifth harmonic of which was zero-beat to the R-band signal. The counter was also used in conjunction with an NMR fluxmeter for accurate determination of the magnetic field.

The absorption measurements were made using a Cary model 14 spectrophotometer and a cold-finger type cryostat designed by H. Hersh and supplied by the H. S. Martin Company. The sample was clamped with a phosphor-bronze leaf spring over a slot in the copper block which forms the bottom of the helium

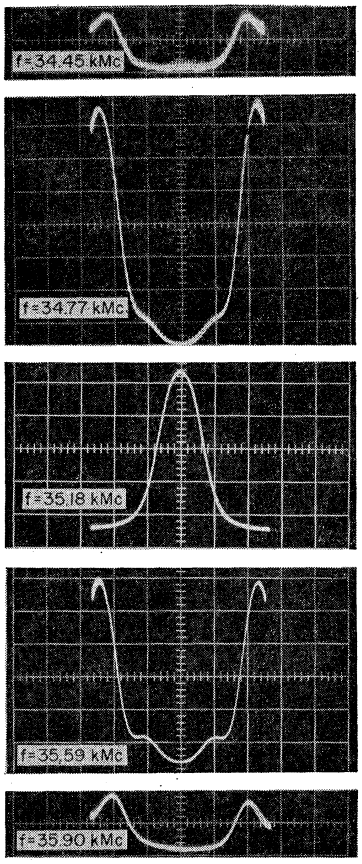

FIG. 5. Ground-state splitting of Cr^{3+} in Ga_2O_3 for zero static magnetic field. The traces show power absorbed by the sample when a sweep field of 310-G peak-to-peak is applied.

reservoir. A series of measurements at room temperature, liquid-nitrogen temperature, and liquid-helium temperature were taken without removing the sample from the cryostat to allow quantitative comparison of the three traces. This precaution was necessary because of inhomogeneous chromium concentration in the samples and the difficulty of reproducing the part of the crystal through which the light beam passed.

Fluorescence measurements were performed using a 1-m Jarrell-Ash high resolution spectrometer. The grating has 7500 lines/in. and is blazed such that, for wavelengths near 7000 Å, the instrument operates in eight order. Light from either a 150-W projector lamp or an AH6 high-pressure mercury arc was used to excite the samples. The light passed through a water filter and then through a blue-green glass color filter that peaks at approximately the same wavelength as the blue absorption of Cr^{3+} in Ga_2O_3. The fluorescent light was filtered with a red glass color filter and focused on the entrance slit of the Jarrell-Ash spectrometer.

IV. EXPERIMENTAL RESULTS

The results of the zero-field measurements are shown in the oscilloscope traces of Fig. 5. These photographs are traces of reflected power versus magnetic field for the R-band spectrometer described previously. In each case, the total sweep amplitude is 310 G. Frequency increases from the top to the bottom trace. For the center trace, f equals W_0 and all four resonance lines coalesce. The two traces adjacent to the center one are for an f greater and less than W_0 by equal amounts. This corresponds to the case shown in Fig. 4, analyzed previously. All four lines are clearly apparent. The top and bottom traces are for a somewhat larger departure of f from W_0, and again f differs from W_0 by equal amounts on each side of W_0. In this case, the sweep is insufficient to enable the outer lines to be observed, since the lines closest to $H=0$ have shifted out to the sweep extremity. Approximate values for D, E, and W_0 follow immediately from such a set of measurements by use of Eq. (5) or the equivalent, if the crystal orientation is known. In attempting to adjust f to equal W_0, it is difficult to see a difference in the trace for very small changes in f near W_0. Therefore, for an accurate measurement of W_0, the peak separation for the $-\frac{3}{2}\rightarrow+\frac{3}{2}$ and $-\frac{1}{2}\rightarrow+\frac{1}{2}$ resonances for several frequencies on each side of W_0 was determined. The peak separation was then plotted versus f; the point of intersection gives W_0, which was found to be 35.178 $\pm$0.005 kMc/sec.

The complete set of spin Hamiltonian parameters was calculated from the X-band measurements. Resonance fields were determined at several frequencies for **H** parallel to the z axis and at the extrema of the curves in Fig. 3. The spin Hamiltonian parameters were then allowed to vary in the expressions relating f and H for these special directions until a self-consistent set was obtained. For the z axis along [010] the results are

$$D=-14.009\pm0.005\ \text{kMc/sec},$$
$$E=+6.142\pm0.005\ \text{kMc/sec},$$
$$g_x=1.978\pm0.001,$$
$$g_y=1.978\pm0.001,$$
$$g_z=1.983\pm0.001.$$

The excellent agreement of measured and calculated values is shown in Fig. 3. The solid curves represent theoretical values for the complete spectrum calculated from the spin Hamiltonian using the above parameters. The data points represent experimental results obtained at room temperature and at the same frequency for which the calculations were made. A set of measurements taken at 34.77 kMc/sec was also in excellent agreement with the values calculated at this frequency using the above spin Hamiltonian. The information contained in the spin Hamiltonian is best summarized in the curves of Fig. 2, which show the splitting of the energy levels versus magnetic field for the field along the principal axes. The approximate angular spectrum for any frequency can easily be sketched from the results presented in Fig. 2.

A typical X-band resonance has a linewidth of about 95 G and is almost independent of temperature. Results

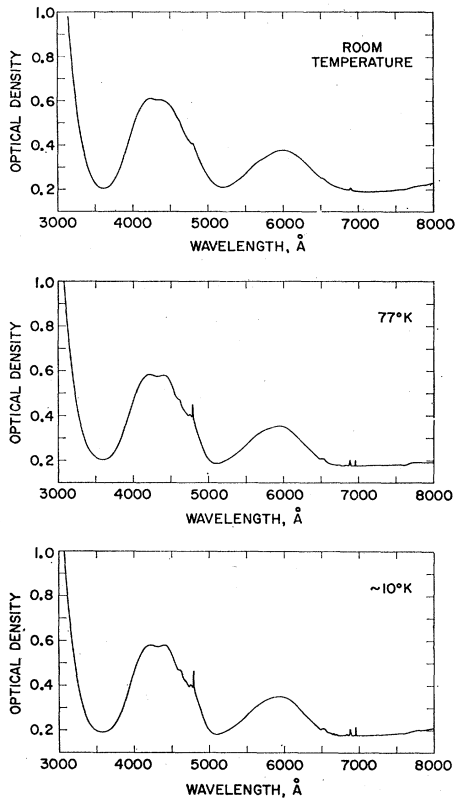

FIG. 6. Absorption spectrum of Cr^{3+} in Ga_2O_3 at several temperatures.

obtained from saturation studies at 2°K and analysis of the line shape suggest that the line is inhomogeneously broadened.

The temperature dependence of D, E, and $\mathbf{g}$ is very small. For a fixed frequency and magnet position, the change in resonance field from room temperature to 2°K is less than one percent. The NMR fluxmeter employed did not permit an accurate determination of the temperature dependence of the spin Hamiltonian parameters.

The absorption spectrum of one of the better samples (from the standpoint of bulk optical quality) is shown in Fig. 6 for three temperatures. This sample is 0.14 cm thick and the faces through which the light passed are (100) planes. Numerous attempts were made to lap and polish the samples in preparation for the absorption measurements, but it was found that the most convenient and effective method was simply to cleave them along two (100) planes. Invariably, the crystals would spontaneously cleave along these planes during attempted polishing operations.

The curves in Fig. 6 were not corrected for multiple internal reflections and are, in fact, raw data traced directly from the Cary model 14 chart recordings. The absorption bands give the crystals a green color, whereas pure Ga_2O_3 is transparent throughout the visible spectrum. Tentative assignments of the excited states involved in the absorption bands and lines were made on the basis of the octahedral field approximation. The octahedral theory gives the position of the energy levels relative to the ground state as a function of B, C, and Dq. The C/B ratio depends very little on n for all the $3d^n$ ions and even less on the environment of a given ion. The value $C/B=4.5$, given by Tanabe and Sugano,[4] was therefore assumed, and values of B and Dq were sought to fit the experimental data to the octahedral theory. The resulting B of 700 cm^{-1} was used to replot the 77°K absorption spectrum at the right in Fig. 1 with the same vertical energy scale as that used for the theoretical curves. The value of $Dq/B=2.35$ is indicated by a dashed line on the energy level diagram. The intersection of the dashed line with the energy levels should be compared with the position of the absorption peaks. The agreement between the absorption data and the energy level diagram is remarkably good, considering the fact that spin-orbit coupling and the fields of symmetry lower than octahedral are not taken into account for the energy level diagram.

A number of interesting observations can be made by comparing this absorption spectrum with that of ruby. For instance, the fine structure effects arising from the spin-orbit coupling and lower symmetry fields are more pronounced for Ga_2O_3, especially for the $^2T_2$ states. There even seems to be some fine structure observable in the upper band ($^4T_1$) at 77°K and below. These results are to be expected since the distortion of the oxygen octahedron is more severe and more complicated for Ga_2O_3. For the sharp doublet transitions, comparison of the average position of all the lines arising from the same degenerate octahedral level reveals that the positions are almost identical in the two cases (shift less than 100 Å). This is easily understood by noting that the average cation-oxygen separation is almost identical in Ga_2O_3 and sapphire, and, in addition, the slope of the doublet levels is very small. The bands, on the other hand, are shifted to the red and broadened for Ga_2O_3. This is to be expected because of the large slope of the quartet levels. A particularly good comparison of the relative shift of the doublet and quartet levels can be obtained by noting the shift of the $^2T_2$ state relative to the $^4T_1$ band. For ruby, the $^2T_2$ transition occurs at the minimum almost exactly midway between the two bands. For Ga_2O_3, the upper band has shifted downward sufficiently to place the $^2T_2$ transition well into its long-wavelength shoulder. A similar situation occurs but to less extent with the ^2E and $^2T_1$ levels relative to the $^4T_2$ band. These effects tend to further enhance the influence of spin-orbit forces and crystal field perturbations of lower symmetry.

The absorption spectrum of nominally pure Ga_2O_3 was also studied at room temperature and at liquid-nitrogen temperature to determine whether it con-

contributed to the net absorption shown in Fig. 6. No absorption was observed between 8000 and 3000 Å, as the visible transparency indicates. At approximately 2800 Å, there is a steep edge, characteristic of a band-to-band transition. This edge undergoes a blue shift of approximately 100 Å when the temperature is reduced to 77°K. It is therefore safe to ignore the optical spectrum of the host material in interpreting the Cr^{3+} data. Some fine structure is present in the edge; this could be due to residual impurities or perhaps exciton effects. Further study of thin samples will be undertaken to clarify this point. It would also be interesting to investigate whether the edge absorption is accompanied by photoconductivity. This could definitely establish that a band-to-band transition is involved and give further information on the existence of excitons.

The positions and half-widths of the R-line fluorescence of Cr^{3+} in Ga_2O_3 as a function of temperature are summarized in Table I. At room temperature, the lines

TABLE I. Positions and widths of R-line fluorescence for Cr^{3+} in β-Ga_2O_3.

	R_1		R_2	
Temperature	Position Å	Half-width Å	Position Å	Half-width Å
Room	6900	24	6966	40
77°K	6883	10	6955.	3
4°K	···	···	6955	1.5

are very broad and incompletely resolved. At 4.2°K, it was not possible to resolve the ground-state splitting of the R_2 line. The ground-state splitting of 35.18 kMc/sec should produce a peak separation of 0.57 Å for the R_2 line. The residual linewidth of the components is too large to permit such a splitting to be resolved. Since Peter and Schawlow[2] have reported that the ground-state splitting could be resolved at 4.2°K in their flux-grown samples, similar samples produced in this laboratory were investigated. It was expected that the linewidth of the flux samples would be smaller than that of an equivalent flame-grown sample because of lower inhomogeneous internal strain. The flux samples, however, had a linewidth approximately twice that of the flame-grown samples, and, again, the ground-state splitting was not resolved. It seems probable, therefore, that the lines are broadened by pair interactions, as is the case in concentrated ruby. Lines resembling the pair spectra reported for ruby have been observed in the Ga_2O_3 fluorescence but have not been investigated in detail. The concentration of the samples can only be estimated, but it is probably a few tenths of one percent. This concentration should be sufficient to produce the observed broadening.

The fluorescence lifetime of the metastable ^2E level was investigated by exciting a crystal with a flash tube strobe unit. The emitted light was observed through an interference filter with a photomultiplier tube, and the signal was displayed on an oscilloscope. The observed decay times were 0.23, 2.8, and 3.5 msec, respectively, at room temperature, 77 and 4.2°K. Interpretation of the low-temperature measurements is complicated by the fact that trapping of the resonance radiation is believed to occur. Another sample consisting of approximately 50 small crystals with a total volume approximately the same as the first sample was also studied. The observed decay times in this case were 0.22 and 1.7 msec at room temperature and 77°K, respectively. The reduced 77°K decay time suggests the need for further experiments to determine whether radiation trapping actually occurs. In this connection, it would be perferable to begin with a single crystal and examine the effect on the 77°K decay time produced by breaking the crystal into smaller and smaller pieces, finally ending up with a fine dispersed powder. For a large ruby, radiation trapping can account for an ob-observed decay time four times as long as that of the state lifetime.[7] The results obtained for the Ga_2O_3 crystal suggest that either the trapping effects are much more pronounced than for ruby or that the ^2E lifetime for Ga_2O_3 has a substantially greater temperature dependence.

The fluorescence efficiency of crystals grown from different starting materials varied considerably. In fact, for most samples, no fluorescence could be observed. The best fluorescing crystal, and the one used for the fluorescence measurements reported here, was grown from material suspected of containing significant foreign impurity concentration in addition to the chromium. It is also a curious fact that the crystals that did not fluoresce exhibited severe losses at X-band frequencies independent of magnetic field. These losses were sufficient even for the smallest samples to lower the cavity Q considerably. Without exception, samples that fluoresced appreciably did not exhibit this anomalous lossy behavior. There is some evidence to support the speculation that the presence of iron impurities is responsible for these effects. The EPR spectrum of iron in Ga_2O_3 was studied in samples that nominally contained only iron. From these results, the presence of iron in the sample that fluoresced well was established. A chromium-doped crystal to which some iron was intentionally added exhibited some fluorescence, but the efficiency was considerably below that of the best crystal. Further studies are required to more completely understand the fluorescence process in this material and to determine the conditions that favor high fluorescence efficiency.

The results of the paramagnetic resonance experiments and calculations suggest that Cr^{3+} in Ga_2O_3 might be successfully employed as the active material for a microwave maser operating at frequencies up to about 50 kMc/sec. However, a difficulty in obtaining

[7] F. Varsanyi, D. L. Wood, and A. L. Schawlow, Phys. Rev. Letters 3, 544 (1959).

large single crystals is encountered. Although boules several grams in weight are readily produced, Ga_2O_3 has a strong tendency to twin in the growth process. This results in samples built up of small needle-like single crystals, some of which have their b axis in one direction, and the remainder their b axis in the opposite direction. Even if large single crystals cannot be produced, it may be possible to overcome this difficulty by judicious choice of sample orientation. The possibility of using Cr^{3+} in Ga_2O_3 as the active material in an optical maser is somewhat less promising, although well worth considering. All of the required characteristics are present to some extent. The linewidth of a few Å is greater than would be desired but could possibly be reduced by almost an order of magnitude with refinements in crystal preparation techniques. Experiments to determine the factors that so strongly affect the quantum efficiency would also be required for perfecting the growth technique. However, it is significant that the quantum efficiency of the best fluorescing samples produced to date is not very different from that of ruby. Another important consideration is whether R-line light is absorbed by the excited system. Experimental investigation of this question has not been performed. On the basis of experiments completed at this time, with the sample quality presently available and the difficulty of fabricating a laser rod, it appears that the operation of this system as a laser would be marginal, at best.

ACKNOWLEDGMENTS

The author is indebted to M. Birnbaum for his efforts in initiating the program to grow Ga_2O_3 and for helpful discussions during the course of this investigation. He is especially indebted to A. Chase for growing the crystals on which most of the work was performed and for his continued interest in this program. The contribution of J. Rowen for supplying the flux grown crystals on which some of the earlier experiments were performed is gratefully acknowledged. Thanks are also due P. Kisliuk for discussions that were valuable in interpreting some of the data and to G. Wolton for his patient explanation of several aspects of the Ga_2O_3 crystal structure.

PHYSICAL REVIEW VOLUME 137, NUMBER 3A 1 FEBRUARY 1965

Electronic Band Structure of Arsenic. I. Pseudopotential Approach*

L. M. Falicov and Stuart Golin

Department of Physics and Institute for the Study of Metals, University of Chicago, Chicago, Illinois

(Received 17 August 1964)

The electronic band structure of arsenic is studied by means of a pseudopotential approach. The pseudopotential has been chosen by (a) fitting the "atomic" pseudopotential of Ge to a four-parameter curve and (b) adjusting the parameters slightly so as to allow comparison of the various theoretical curves with the experimental data. The energy bands are determined by diagonalizing a fairly large ($\approx 90 \times 90$) secular determinant. Spin-orbit coupling is included *a posteriori*. Group-theoretical analysis is carried out throughout the Brillouin zone and use is made of the classification of the levels as well as the compatibility relations. It is found that the holes are located at T, the center of the hexagonal face. The electrons are probably distributed in six equivalent pockets, each one located along a binary axis in a pseudohexagonal face, near its center L.

1. INTRODUCTION

THE group-V semimetals, As, Sb, and Bi, have been for a long time the center of interest of many investigators both from the theoretical and the experimental points of view.[1] The main reason behind this wide interest lies in the fact that a small effective number of carriers makes transport and equilibrium properties relatively easy to measure as well as easy to interpret in terms of a few parameters.

However the over-all band structure of the semimetals has remained, up to now, virtually untouched. This is so because the small number of effective carriers is in this case a drawback rather than an advantage, since only a minute region of the Brillouin zone can be reached by the standard experimental techniques. In addition the relatively low symmetry of the A7 (arsenic) structure complicates the theoretical approach. But without a reasonable overall energy-level diagram, complicated experimental measurements like optical properties[2] or behavior upon alloying[3] cannot be reliably interpreted.

Of the three group-V semimetals, arsenic is the one

* Work supported in part by the National Science Foundation and the U. S. Office of Naval Research.

[1] For a summary of the present state of the many facets of the field see, for instance, the proceedings of the Topical Conference on Semimetals, New York, IBM J. Res. Develop. 8, 215 (1964), and the many references quoted there.

[2] M. Cardona and D. L. Greenaway, Phys. Rev. 133, A1685 (1964).

[3] See Ref. 1 for work on Bi-Sb alloys and for further references.

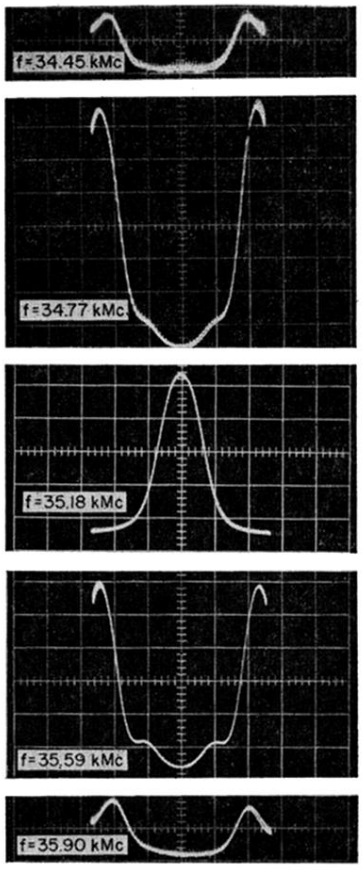

FIG. 5. Ground-state splitting of Cr^{3+} in Ga_2O_3 for zero static magnetic field. The traces show power absorbed by the sample when a sweep field of 310-G peak-to-peak is applied.